Numerical Simulation and Prediction for Steep Water Gravity Waves of Arbitrary Uniform Depth using Artificial Neural Network

Mostafa A. M. Abdeen mostafa_a_m_abdeen@hotmail.com
Faculty of Engineering/Dept. of Engineering Mathematics and Physics
Cairo University Giza, 12211, Egypt

Samir Abohadima s@abohadima.com
Faculty of Engineering/Dept. of Engineering Mathematics and Physics
Cairo University Giza, 12211, Egypt

Abstract

Nonlinear permanent progressive wave is one of the most important applications in water waves. In this study, analytic formulation of the steep water gravity waves is presented. Abohadima and Isobe [1] showed that Cokelet solution [2] is the most accurate among many other solutions. Due to the nonlinearity of analytic equations, the need to numeric simulation is raised up. In the current paper, consequence numerical models, using one of the artificial intelligence techniques, are designed to simulate and then predict the non linear properties of permanent steep water waves. Artificial Neural Network (ANN), one of the artificial intelligence techniques, is introduced in the current paper to simulate and predict the wave celerity, momentum, energy and other wave integral properties for any permanent waves in water of arbitrary uniform depth. The ANN results presented in the current study showed that ANN technique, with less effort, is very efficiently capable of simulating and predicting the non linear properties of permanent steep water waves.

Keywords: Steep water gravity waves; Nonlinear permanent progressive wave; Numerical simulation; Artificial Neural Network.

1. INTRODUCTION

The Nonlinear permanent progressive wave is one of the most important applications in water waves. Although, the problem boundary conditions are simple, however wave nonlinearity is main source of complexity especially near limiting waves. For calculating the integrated properties of nonlinear waves, various nonlinear wave theories are used. Dean [3, 4], Chaplin [5], and Rienecker and Fenton [6] used the stream function wave theory while Longuet-Higgins and Fenton [7], Schwartz [8], Longuet-Higgins [9], and Cokelet [2] used higher order perturbation techniques with different expansion parameters. Yamada and Shiotani [10] used complete integral functions. Abohadima and Isobe [1] showed that Cokelet solution [2] is the most accurate among many other solutions, however the solution was very complicated.

Due to complexity of Cokelet solution, The ANN was examined in this article to get solution at any wave conditions and to keep the same level of Cokelet accuracy. Artificial intelligence has proven its capability in simulating and predicting the behavior of the different physical phenomena in most of the engineering fields. ANN is one of the artificial intelligence techniques that have been incorporated in various scientific disciplines. Minns [11] investigated the general application of ANN in modeling rainfall runoff process. Kheireldin ([12] presented a study to model the hydraulic characteristics of severe contractions in open channels using ANN technique. The successful results of his study showed the applicability of using the ANN approach in determining

relationship between different parameters with multiple input/output problems. Abdeen [13] developed neural network model for predicting flow characteristics in irregular open channels. The developed model proved that ANN technique was capable with small computational effort and high accuracy of predicting flow depths and average flow velocities along the channel reach when the geometrical properties of the channel cross sections were measured or vice versa. Allam [14] used the artificial intelligence technique to predict the effect of tunnel construction on nearby buildings, which is the main factor in choosing the tunnel route. Abdeen ([15] presented a study for the development of ANN models to simulate flow behavior in open channel infested by submerged aquatic weeds. Mohamed [16] proposed an artificial neural network for the selection of optimal lateral load-resisting system for multi-story steel frames. Abdeen [17] utilized ANN technique for the development of various models to simulate the impacts of different submerged weeds' densities, different flow discharges, and different distributaries operation scheduling on the water surface profile in an experimental main open channel that supplies water to different distributaries. Abdeen et al. [18] introduced the ANN technique to investigate the effect of light local weight aggregate on the performance of the produced lightweight concrete. The results of their study showed that the ANN method with less effort was very efficiently capable of simulating the effect of different aggregate materials on the performance of lightweight concrete. Hodhod et al. [19] introduced the ANN technique to simulate the strength behavior using the available experimental data and predict the strength value at any age in the range of the experiments or in the future. The results of the numerical study showed that the ANN method was very efficiently capable of simulating the effect of specimen shape and type of sand on the strength behavior of tested mortar with different cement types.

2. AIM OF THE WORK

The analytic formulation for the steep water gravity waves is presented in details. The Cokelet analytic solution is described in the present work and is considered the most accurate among many other solutions. Consequence numerical models are developed in the current work, using ANN technique, to understand, simulate and predict, the wave celerity, momentum, energy and other wave integral properties for any permanent waves in water of arbitrary uniform depth.

3. ANALYTICAL FORMULATION

Consider two dimensional, periodic, surface waves of wavelength λ and wave number $k=2\pi/\lambda$ propagating under the influence of gravity, g, in the fluid of constant density, ρ. Take units of mass, length and time such that $k = \rho = g = 1$ and hence $\lambda = 2\pi$. Assume that the fluid is inviscid and incompressible and the flow is irrotational. The waves are assumed to flow from left to right over a horizontal bottom without change in form. By a choice of reference frame, the fluid velocity at any fixed depth always within the fluid averaged over one wave cycle may be taken as zero. The frame of reference is unique as is the propagation speed, c, of the waves with respect to that frame.

Choose rectangular coordinates (x, y) such that the x-axis is horizontal and the y-axis is directed vertically upwards. Locate the free surface at $y= \eta$ and the bottom at $y=-d$ where d is referred to the undisturbed fluid depth and represents the depth of a uniform stream flowing with speed c whose mass flux, $Q= c\ d$ equals that of the wave. The mean elevation of the free surface is $\overline{\eta}$ where an over bar denotes an average over one wave cycle. Therefore the mean depth is $D=d+\overline{\eta}$ and does not in general equal-to-equal d. Since the fluid is irrotational and incompressible, a velocity potential, ϕ, and stream function, ψ, can be defined such that the velocity, (u, v), may be written as follows:

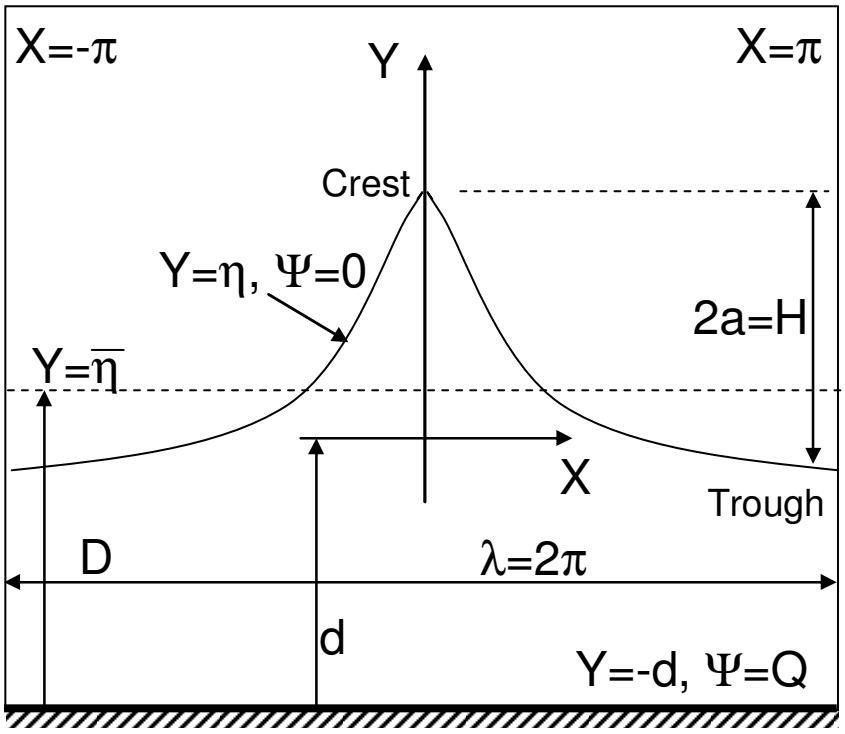

FIGURE 1: Wave Profile in Z-Plane

$$\left.\begin{aligned} u &= \frac{\partial \phi}{\partial x} = \frac{\partial \psi}{\partial y} \\ v &= \frac{\partial \phi}{\partial y} = -\frac{\partial \psi}{\partial x} \end{aligned}\right\} \tag{1}$$

And both ϕ and ψ satisfy Laplace's equation, $\nabla^2\phi = \nabla^2\psi = 0$

Now considering a second rectangular coordinate system (*X, Y*) moving in the positive x-direction with the waves at speed *c*, In this reference frame the motion is independent of time, t. The velocity potential, Φ, stream function, Ψ, and velocity (*U, V*), in this frame are related to similar quantities in the (*x, y*) frame by:

$$\left.\begin{aligned} & X = x - ct, \qquad Y = y, \quad \Phi = \phi - cx, \quad \Psi = \psi - cy \\ & U = u - c = \frac{\partial \Phi}{\partial X} = \frac{\partial \Psi}{\partial Y} \\ & V = v = \frac{\partial \Phi}{\partial Y} = -\frac{\partial \psi}{\partial X} \end{aligned}\right\} \tag{2}$$

It is convenient to define the complex variables $Z=X+iY$ and $W=\Phi+i\Psi$ which are analytic functions of one another. The *Z*-plane is shown in Figure (1)

The boundary conditions to be imposed on the flow are that the free surface and bottom are streamlines, that is

$$\left.\begin{aligned} \Psi = 0 \quad on \qquad Y = \eta \\ \Psi = Q \quad on \qquad Y = -d \end{aligned}\right\} \tag{3}$$

In addition, the pressure along the free surface is assumed to be equal to the constant atmospheric pressure (ρ=0) with the effects of surface tension neglected. So the Bernoulli equation at the free surface becomes:

$$U^2 + V^2 + 2\eta = K \quad \text{on } \Psi=0, \tag{4}$$

Where *K* is the Bernoulli constant in the moving coordinates system.

Following Cokelet, by taking Z as a Fourier series in *W* of the form

$$Z(W) = A_o \frac{W}{c} + B_o + \sum_{j=1}^{\infty} \left(A_j \, e^{ijW/c} + B_j \, e^{-ijW/c} \right) \tag{5}$$

Applying the bottom boundary condition (3) and the fact that wave profile must be symmetric, Equation (5) will simplified to

$$X = -\frac{\Phi}{c} - \sum_{j=1}^{\infty} \frac{a_j}{j} \left(e^{-j\Psi/c} + e^{-2jd} e^{j\Psi/c} \right) Sin\left(j \frac{\Phi}{c} \right) \tag{6}$$

$$Y = -\frac{\Psi}{c} + \sum_{j=1}^{\infty} \frac{a_j}{j} \left(e^{-j\Psi/c} - e^{-2jd} e^{j\Psi/c} \right) Cos\left(j \frac{\Phi}{c} \right) \tag{7}$$

The real constant a_j in equations (6) and (7) are determined by satisfying the Bernoulli equation (4) on the free surface. The complex velocity, q, is given by

$$q = U - iV = \frac{dW}{dZ} = \left(\frac{dZ}{dW} \right)^{-1} = \frac{-c}{1 + \sum_{j=1}^{\infty} a_j \left(e^{-ijW/c} + e^{-2jd} e^{-ijW/c} \right)} \tag{8}$$

Substitution of (6), (7) and (8) into (4) gives

$$c^2 + \left\{ 2 \sum_{j=1}^{\infty} \frac{a_j}{j} \delta_j \, Cos\left(j \frac{\Phi}{c} \right) - K \right\} \left\{ \begin{aligned} &\left[1 + \sum_{j=1}^{\infty} a_j \, \sigma_j \, Cos\left(j \frac{\Phi}{c} \right) \right]^2 \\ &+ \left[\sum_{j=1}^{\infty} a_j \, \delta_j \, Sin\left(j \frac{\Phi}{c} \right) \right]^2 \end{aligned} \right\} = 0 \tag{9}$$

Where two parameters depending only on *d* and defined by

$$\sigma_j = 1 + e^{-2jd}, \qquad \delta_j = 1 - e^{-2jd} \tag{10}$$

Expanding equation (9) as a cosine series and equating the harmonic coefficients to zero, we get:

$$\left.\begin{aligned} &c^2 + 2 \sum_{n=1}^{\infty} \frac{a_n}{n} \delta_n f_1 = K f_o, \\ &\sum_{n=1}^{\infty} \frac{a_n}{n} \delta_n \left(f_{|n-j|} + f_{n+j} \right) = K f_j \quad (j = 1, 2, ...) \end{aligned}\right\} \tag{11}$$

Where f_j have been introduced for convenience and are defined in terms of the a_j by

$$\left.\begin{aligned} f_o &= 1+\sum_{n=1}^{\infty} a_n^2\,\sigma_{2n}, \\ f_j &= a_j\sigma_j+\sum_{n=1}^{\infty} a_n a_{n+j}\sigma_{2n+j}+\frac{1}{2}\sum_{n=1}^{j-1} a_n a_{j-n}\left(\sigma_n-\delta_{j-n}\right) \quad (j=1,2,....) \end{aligned}\right\} \tag{12}$$

In all summations, each term is taken to be identical zero if the lower limit exceeds the upper.

Equations (11) and (12) are a set of nonlinear algebraic equations that determine the Fourier coefficients a_j completely. These can be solved in a consistent manner by perturbation expansion technique. Let ε denote a global perturbation parameter, which is zero for infinitesimal waves and is positive for higher waves.

$$\left.\begin{aligned} a_j &= \sum_{k=0}^{\infty}\alpha_{jk}\varepsilon^{j+2k}, \quad (j=1,2,.....) \\ f_j &= \sum_{k=0}^{\infty}\beta_{jk}\varepsilon^{j+2k}, \quad (j=1,2,.....) \\ c^2 &= \sum_{n=0}^{\infty}\gamma_n\varepsilon^{2n} \\ K &= \sum_{n=0}^{\infty}\Delta_n\varepsilon^{2n} \end{aligned}\right\} \tag{13}$$

Substituting of (13) into (11) and (12), then equating coefficients of equal powers of ε yields the following recurrence relations:

$$\gamma_n+2\sum_{j=0}^{n-1}\frac{\delta_{n-j}}{n-j}\sum_{m=0}^{j}\alpha_{n-j,j-m}\beta_{n-j,m}=\sum_{k=0}^{n}\Delta_{n-k}\beta_{0k}, \quad (n=0,1,2,.....) \tag{14}$$

$$\begin{aligned} \sum_{n=0}^{p}\Delta_n\beta_{j,p-n} &= \sum_{n=1}^{j}\frac{\delta_n}{n}\sum_{k=0}^{p}\alpha_{n,p-k}\beta_{j-n,k}+\sum_{n=1}^{p}\frac{\delta_{n+j}}{n+j}\sum_{k=0}^{p-n}\alpha_{n+j,p-n-k}\beta_{nk} \\ &+\sum_{n=0}^{p-1}\frac{\delta_{p-n}}{p-n}\sum_{k=0}^{n}\alpha_{p-n,n-k}\beta_{j+p-n,k} \quad , \quad (j=1,2,...;p=0,1,...) \end{aligned} \tag{15}$$

$$\beta_{00}=1 \tag{16}$$

$$\beta_{0k}=\sum_{n=0}^{k}\sigma_{2n}\sum_{p=0}^{k-n}\alpha_{np}\alpha_{n,k-n-p} \quad , \quad (k=0,1,2,.....) \tag{17}$$

$$\begin{aligned} \beta_{jk} &= \alpha_{jk}\sigma_j+\frac{1}{2}\sum_{n=1}^{j-1}\left(\sigma_j-\delta_{j-n}\right)\sum_{p=0}^{k}\alpha_{np}\alpha_{j-n,k-p} \\ &+\sum_{n=1}^{k}\sigma_{2n+j}\sum_{p=0}^{k-n}\alpha_{np}\alpha_{n+j,k-n-p} \quad , \quad (j=1,2,...;k=0,1,...) \end{aligned} \tag{18}$$

Cokelet selected the expansion parameter ε as follow:

$$\varepsilon^2=1-\frac{q_{crest}^2 q_{trough}^2}{c^4} \tag{19}$$

The fluid speeds at the wave crest and trough are obtained from (8) with Ψ=0 and Φ/c=0 and π respectively. Expanding the right hand side of (19) in powers of ε leads to:

$$\varepsilon^2 = 1 - \frac{1}{\left(1+\sum_{j=1}^{\infty}\sum_{k=0}^{\infty}\sigma_j \alpha_{jk}\varepsilon^{j+2k}\right)^2 + \left(1+\sum_{j=1}^{\infty}\sum_{k=0}^{\infty}(-1)^j \sigma_j \alpha_{jk}\varepsilon^{j+2k}\right)^2} \tag{20}$$

Rearrange and expanding (20) and equating powers of ε gives

$$\begin{aligned}
&\frac{(-1)^j\left(-\frac{1}{2}\right)!}{j!\left(-j-\frac{1}{2}\right)!} = 2\sum_{k=0}^{j-1}\alpha_{2(j-k),k}\sigma_{2(j-k)} \\
&+\sum_{n=1}^{j-1}\sum_{k=0}^{j-n-1}\sum_{m=0}^{j-n-k-1}\sigma_{2(j-n-k-m)}\sigma_{2n}\alpha_{2(j-n-k-m),k}\alpha_{2n,m} \\
&-\sum_{n=0}^{j-1}\sum_{k=0}^{j-n-1}\sum_{m=0}^{j-n-k-1}\sigma_{2(j-n-k-m)-1}\sigma_{2n+1}\alpha_{2(j-n-k-m)-1,k}\alpha_{2n+1,m}
\end{aligned} \tag{21}$$

The calculation procedure is as follows:

1- Specify the maximum order, N, of the perturbation expansion,
2- Specify the undisturbed fluid depth, d, and calculate δ_j σ_j using (10)
3- Calculate the coefficient at order ε^p in terms of the previously determined coefficients with p=0, 1,….., 2M, 2M+1, …., N
(a) Within any even order, 2M,
(i) Calculate α_{ij} and β_{ij} by solving equations (15) and (17) simultaneously proceeding in the sequence (i,j)=(2M,0), (2M-2,1), ….,(4,M-2)
(ii) Calculate $\alpha_{1,M-1}$, $\beta_{1,M-1}$, $\alpha_{2,M-1}$, and $\beta_{2,M-1}$ by simultaneously solving equations (17) with j=1, k=M-1, (15) with j=2, p=M-1, (17) with j=2, k=M-1, and equations (14) to (18) with j=M,
(iii) Calculate β_{0M} from equation (18) with k=M,
(b) Within any odd order, 2M+1,
(i) Calculate Δ_M from (15) with j=1, p=M
(ii) Calculate α_{ij} and β_{ij} by solving equations (15) and (17) simultaneously proceeding in the sequence (i,j)=(2M+1,0), (2M-1,1), ….,(3,M-1)
4- Calculate γ_n from (14) with n=0, 1,…., $\frac{1}{2}N$

Notice that the odd-order coefficients $\alpha_{1,M-1}$ and $\beta_{1,M-1}$ can not be determined until the next higher order even order, and also that even-order Δ_M can not be determined until the next higher odd order.

After calculation of all coefficients, wave properties can be computed as follows:
the wave hieght,

$$a = \frac{1}{2}H = \sum_{j=1}^{\infty}\frac{1}{2j-1}a_{2j-1}\delta_{2j-1} = \sum_{j=1}^{\infty}\sum_{k=1}^{j}\frac{1}{2j-1}\alpha_{2j-1,j-1}\delta_{2j-1}\varepsilon^{2j-1} \tag{22}$$

$\bar{\eta}$ the mean elevation of free water surface,

$$\bar{\eta} = \frac{1}{2\pi}\int_0^{2\pi} Y\ (\Phi,0)dX = \frac{1}{2}\sum_{j=1}^{\infty}\sum_{k=1}^{j-1}\sum_{n=0}^{j-k-1}\frac{\delta_{j-k-n}\sigma_{j-k-n}}{j-k-n}\alpha_{j-k-n,k}\alpha_{j-k-n,n}\varepsilon^{2j} \tag{23}$$

$$\overline{\eta^2} = \frac{1}{2\pi}\int_0^{2\pi} Y^2(\Phi,0)dX = \frac{1}{2}\sum_{j=1}^{\infty}\sum_{k=0}^{j-1}\sum_{n=0}^{j-k-1}\frac{\delta_{j-k-n}}{(j-k-n)^2}\alpha_{j-k-n,k}\alpha_{j-k-n,n}\varepsilon^{2j} +$$
$$\frac{1}{4}\sum_{j=2}^{\infty}\sum_{m=1}^{j-1}\sum_{k=0}^{j-m-1}\sum_{i=0}^{j-m-k-1}\sum_{n=0}^{j-m-k-i-1}\frac{\delta_{j-m-k-i-n}}{j-m-k-i-n} * \quad (24)$$
$$\left(\frac{\delta_m\sigma_{j-k-i-n}}{m} + 2\frac{\delta_{j-k-i-n}\sigma_m}{j-k-i-n}\right)\alpha_{j-m-k-i-n,k}\alpha_{mi}\alpha_{j-k-i-n,n}\varepsilon^{2j}$$

Table 1 gives all relation required to compute integral properties analytically using the computed coefficients.

Integral propety	Calculation Relation
The circulation per unit length, C	$C = \frac{1}{\lambda}\int_0^{\lambda} u dx = \bar{u}$
The mean momentum or impulse, *I*	$I = \overline{\int_{-d}^{\eta} \rho u dy}$
The kinetic energy, *T*,	$T = \overline{\int_{-d}^{\eta} \frac{1}{2}\rho\left(u^2+v^2\right)dy}$
The potential evergy, *V*	$V = \overline{\int_{\bar{\eta}}^{\eta} \rho g y dy}$
The radiation stress S_{xx}	$S_{xx} = \overline{\int_{-d}^{\eta}\left(p+\rho u^2\right)dy} - \int_{-d}^{\bar{\eta}} p_0 dy$
The mean energy flux, *F*	$F = \overline{\int_{-d}^{\eta}\left(p+\frac{1}{2}\rho\left(u^2+v^2\right)+\rho g\left(y-\bar{\eta}\right)\right)udy}$
The mean squareed velocity at the bottom $\overline{u_b^2}$	$\overline{u_b^2} = \frac{1}{\lambda}\int_0^{\lambda}\left(u[x,-d]\right)^2 dx$
The mass flux per unit span, *Q*	$Q = -\int_{-d}^{\lambda}\rho U dY$
The Bernoulli constant, K	$K = 2\rho\bar{\eta} + \overline{u_b^2} + c^2$
The total head *R*	$R = \frac{1}{2}K + d$
The momentum flux per unit span, *S*	$S = S_{xx} - 2cI + D\left(c^2 + \frac{1}{2}D\right)$

TABLE 1: Relations of integral properties

Where p_o is the hydrostatic pressure defined as follws:

$$p_o = -\rho g\left(y-\bar{\eta}\right) \quad (25)$$

4. NUMERICAL MODEL STRUCTURE

Neural networks (NN) are models of biological neural structures. Abdeen [13] described in a very detailed fashion the structure of any neural network. Briefly, the starting point for most networks is

a model neuron as shown in Fig. 2. This neuron is connected to multiple inputs and produces a single output. Each input is modified by a weighting value (w). The neuron will combine these weighted inputs with reference to a threshold value and an activation function, will determine its output. This behavior follows closely the real neurons work of the human's brain. In the network structure, the input layer is considered a distributor of the signals from the external world while hidden layers are considered to be feature detectors of such signals. On the other hand, the output layer is considered as a collector of the features detected and the producer of the response.

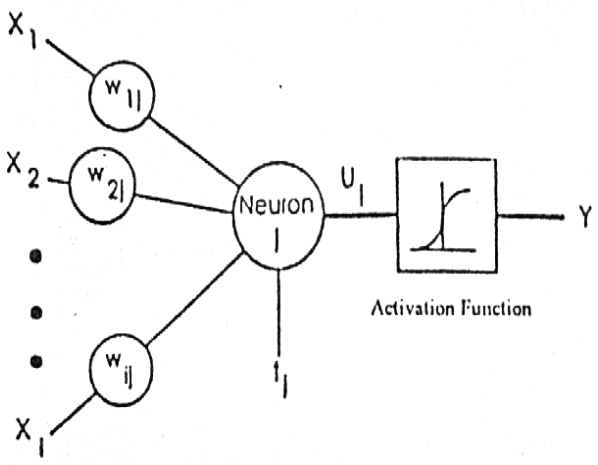

FIGURE 2: Typical picture of a model neuron that exists in every neural network

4.1 Neural Network Operation

It is quite important for the reader to understand how the neural network operates to simulate different physical problems. The output of each neuron is a function of its inputs (X_i). In more details, the output (Y_j) of the j^{th} neuron in any layer is described by two sets of equations as follows:

$$U_j = \sum\left(X_i w_{ij} \right) \tag{26}$$

$$Y_j = F_{th}\left(U_j + t_j\right) \tag{27}$$

For every neuron, *j*, in a layer, each of the *i* inputs, X_i, to that layer is multiplied by a previously established weight, w_{ij}. These are all summed together, resulting in the internal value of this operation, U_j. This value is then biased by a previously established threshold value, t_j, and sent through an activation function, F_{th}. This activation function can take several forms such as Step, Linear, Sigmoid, Hyperbolic, and Gaussian functions. The Hyperbolic function, used in this study, is shaped exactly as the Sigmoid one with the same mathematical representation, as in equation 12, but it ranges from – 1 to + 1 rather than from 0 to 1 as in the Sigmoid one (Fig. 3)

$$f(x) = \frac{1}{1+e^{-x}} \tag{28}$$

The resulting output, Y_j, is an input to the next layer or it is a response of the neural network if it is the last layer. In applying the Neural Network technique, in this study, Neuralyst Software, Shin [20], was used.

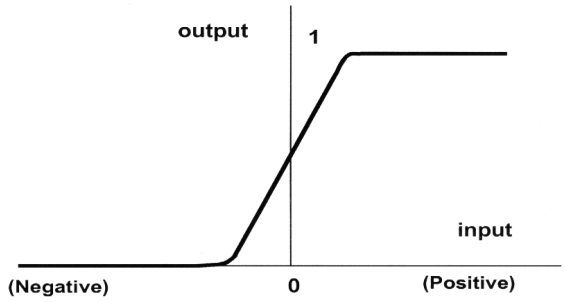

FIGURE 3: The Sigmoid Activation Function

4.2 Neural Network Training

The next step in neural network procedure is the training operation. The main purpose of this operation is to tune up the network to what it should produce as a response. From the difference between the desired response and the actual response, the error is determined and a portion of it is back propagated through the network. At each neuron in the network, the error is used to adjust the weights and the threshold value of this neuron. Consequently, the error in the network will be less for the same inputs at the next iteration. This corrective procedure is applied continuously and repetitively for each set of inputs and corresponding set of outputs. This procedure will decrease the individual or total error in the responses to reach a desired tolerance. Once the network reduces the total error to the satisfactory limit, the training process may stop. The error propagation in the network starts at the output layer with the following equations:

$$w_{ij} = w'_{ij} + LR\left(e_j X_i\right) \tag{29}$$

$$e_j = Y_j\left(1 - Y_j\right)\left(d_j - Y_j\right) \tag{30}$$

Where, w_{ij} is the corrected weight, w'_{ij} is the previous weight value, LR is the learning rate, e_j is the error term, X_i is the i^{th} input value, Y_j is the output, and d_j is the desired output.

5. CONSEQUENCE NUMERICAL MODELS

To fully investigate numerically the wave integral properties for any permanent waves in water of arbitrary uniform depth, five consequence neural network models are designed in this study. Consequence models mean that each model uses the inputs and the outputs of the previous one to be as input variables for the next model to produce another group of outputs and so on until we reach the last one.

5.1 Neural Network Design

To develop neural network models to simulate the water wave integral properties, first input and output variables have to be determined. Input variables are chosen according to the nature of the problem and the type of data that would be collected. To clearly specify the key input variables for each neural network model and their associated outputs, Fig. 4 and Table 2 are designed to summarize all neural network key input and output variables for the five consequence neural network models respectively.

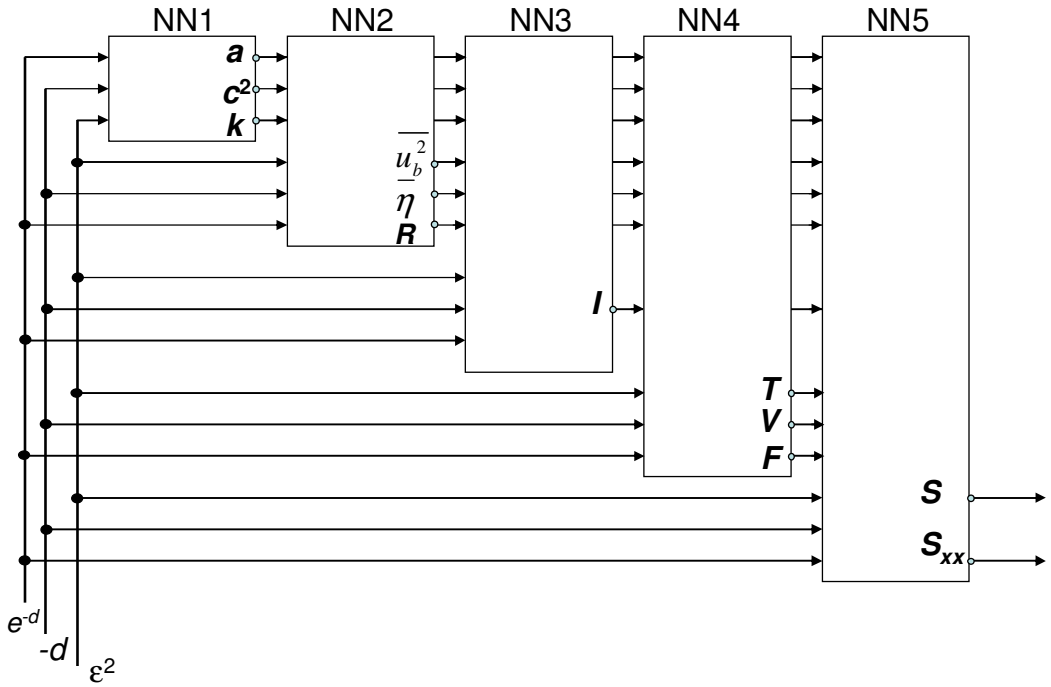

FIGURE 4: Consequence Neural Network Models

Model	e^{-d}	-d	ε^2	a	c^2	k	$\bar{u}^2_b$	$\overline{\eta}$	R	I	T	V	F	S	S_{xx}
NN1	*I*	*I*	*I*	*O*	*O*	*O*	-	-	-	-	-	-	-	-	-
NN2	*I*	*I*	*I*	*I*	*I*	*I*	*O*	*O*	*O*	-	-	-	-	-	-
NN3	*I*	*I*	*I*	*I*	*I*	*I*	*I*	*I*	*I*	*O*	-	-	-	-	-
NN4	*I*	*I*	*I*	*I*	*I*	*I*	*I*	*I*	*I*	*I*	*O*	*O*	*O*	-	-
NN5	*I*	*I*	*I*	*I*	*I*	*I*	*I*	*I*	*I*	*I*	*I*	*I*	*I*	*O*	*O*

Note: *I* denotes for Input Variable and *O* denotes for Output Variable

TABLE 2: Key Input and Output Variables for Neural Network Models

Several neural network architectures are designed and tested for all numerical models investigated in this study to finally determine the best network models to simulate, very accurately, the water wave integral properties based on minimizing the Root Mean Square Error (RMS-Error). Fig. 5 shows a schematic diagram for a generic neural network. The training procedure for the developed NN models, in the current study, uses the data from the results of the analytical model to let the ANN understands the behaviors. After sitting finally the NN models, these models are used to predict the wave properties for different relative fluid depth (d) rather than those used in the analytic solution.

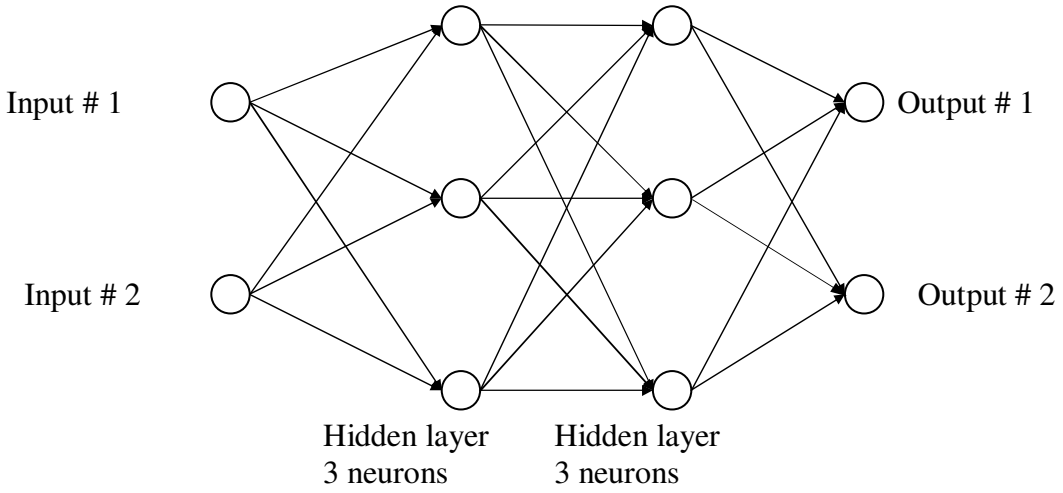

FIGURE 5: General schematic diagram of a simple generic neural network

Table 3 shows the final neural network models for the five consequence models and their associate number of neurons. The input and output layers represent the key input and output variables described previously for each model.

Model	No. of layers	No. of Neurons in each layer			
		Input Layer	First Hidden	Second Hidden	Output Layer
NN1	4	3	5	4	3
NN2	4	6	5	4	3
NN3	4	9	6	4	1
NN4	4	10	8	6	3
NN5	4	13	9	5	2

TABLE 3: The developed Neural Network Models

The parameters of the various network models developed in the current study are presented in Table (4), where these parameters can be described with their tasks as follows:

Learning Rate (LR): determines the magnitude of the correction term applied to adjust each neuron's weights during training process = 1 in the current study.
Momentum (M): determines the "life time" of a correction term as the training process takes place = 0.9 in the current study.
Training Tolerance (TRT): defines the percentage error allowed in comparing the neural network output to the target value to be scored as "Right" during the training process = 0.01 in the current study.
Testing Tolerance (TST): it is similar to Training Tolerance, but it is applied to the neural network outputs and the target values only for the test data = 0.03 in the current study.
Input Noise (IN): provides a slight random variation to each input value for every training epoch = 0 in the current study.
Function Gain (FG): allows a change in the scaling or width of the selected function = 1 in the current study.
Scaling Margin (SM): adds additional headroom, as a percentage of range, to the rescaling computations used by Neuralyst Software, Shin (1994), in preparing data for the neural network or interpreting data from the neural network = 0.1 in the current study.
Training Epochs: number of trails to achieve the present accuracy.

Percentage Relative Error (PRR): percentage relative error between the numerical results and actual measured value for and is computed according to equation (6) as follows:

PRE = (Absolute Value (ANN_PR - AMV)/AMV)*100

Where :

ANN_PR : Predicted results using the developed ANN model

AMV : Actual Measured Value

MPRE : Maximum percentage relative error during the model results for the training step (%)

Simulation Parameter	NN1	NN2	NN3	NN4	NN5
Training Epochs	225823	256762	30077	5325	11004
MPRE	3.5	4.4	5.3	4.8	5.7
RMS-Error	0.0038	0.0079	0.0036	0.0035	0.0028

TABLE 4: Parameters used in the Developed Neural Network Models

6. RESULTS AND DISCUSSIONS

Numerical results using ANN technique will be presented in this section for the five consequence neural network models (NN1—NN5) to show the simulation and prediction powers of ANN technique of wave celerity, momentum, energy and other wave integral properties for any permanent wave in water of arbitrary uniform depth.

Figures (6—9) show a comparison between ANN results (dotted lines) and analytical results (symbols) for a, c^2, K, $\overline{\eta}$, $\overline{u_b^2}$, R, I, T, V, F, S_{xx} and S at different undisturbed fluid depths and wave nonlinearity parameters. Square symbols used in training phase, and triangle symbols used to show the power of prediction of neural network models developed in the present work. It is very clear, from these figures, that the developed neural network models are very efficiently capable of simulating and predicting the non linear properties of permanent steep water waves.

7. CONCLUSIONS

Based on the results of implementing the ANN technique in this study, the following can be concluded:

1. The developed consequence neural network models, presented in this study, are very successful in simulating the non linear properties of permanent steep water waves.
2. The presented neural network models are very efficiently capable of predicting the properties of water waves at different undisturbed fluid depths and wave nonlinearity parameters rather than those used in the training step for developing the models.

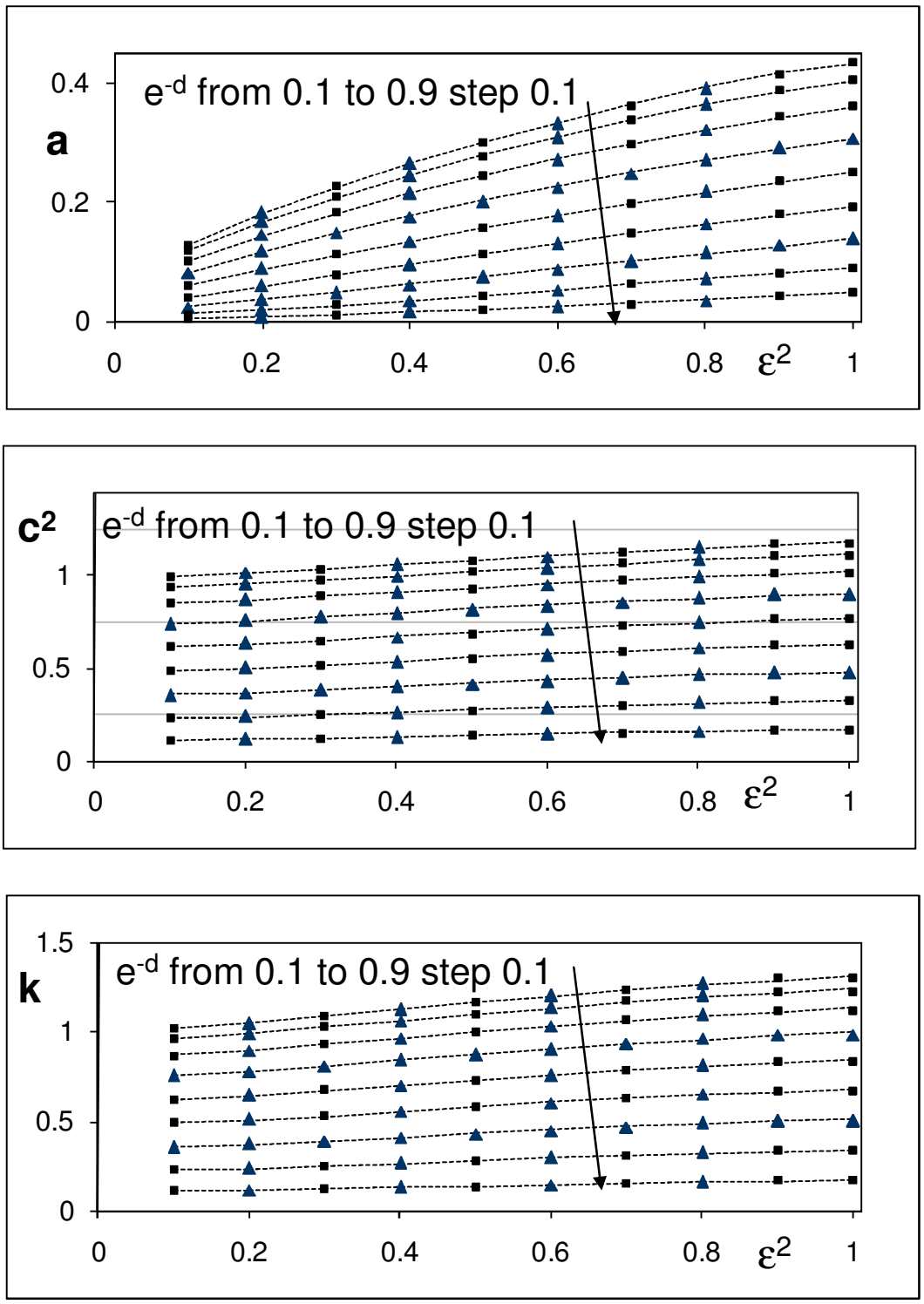

FIGURE 6: Comparison between ANN (dotted lines) and analytical results (symbols) for *a*, c^2 and *K* at different undisturbed fluid depths and wave nonlinearity parameters. Square symbols used in training phase, and triangle symbols used only for comparison

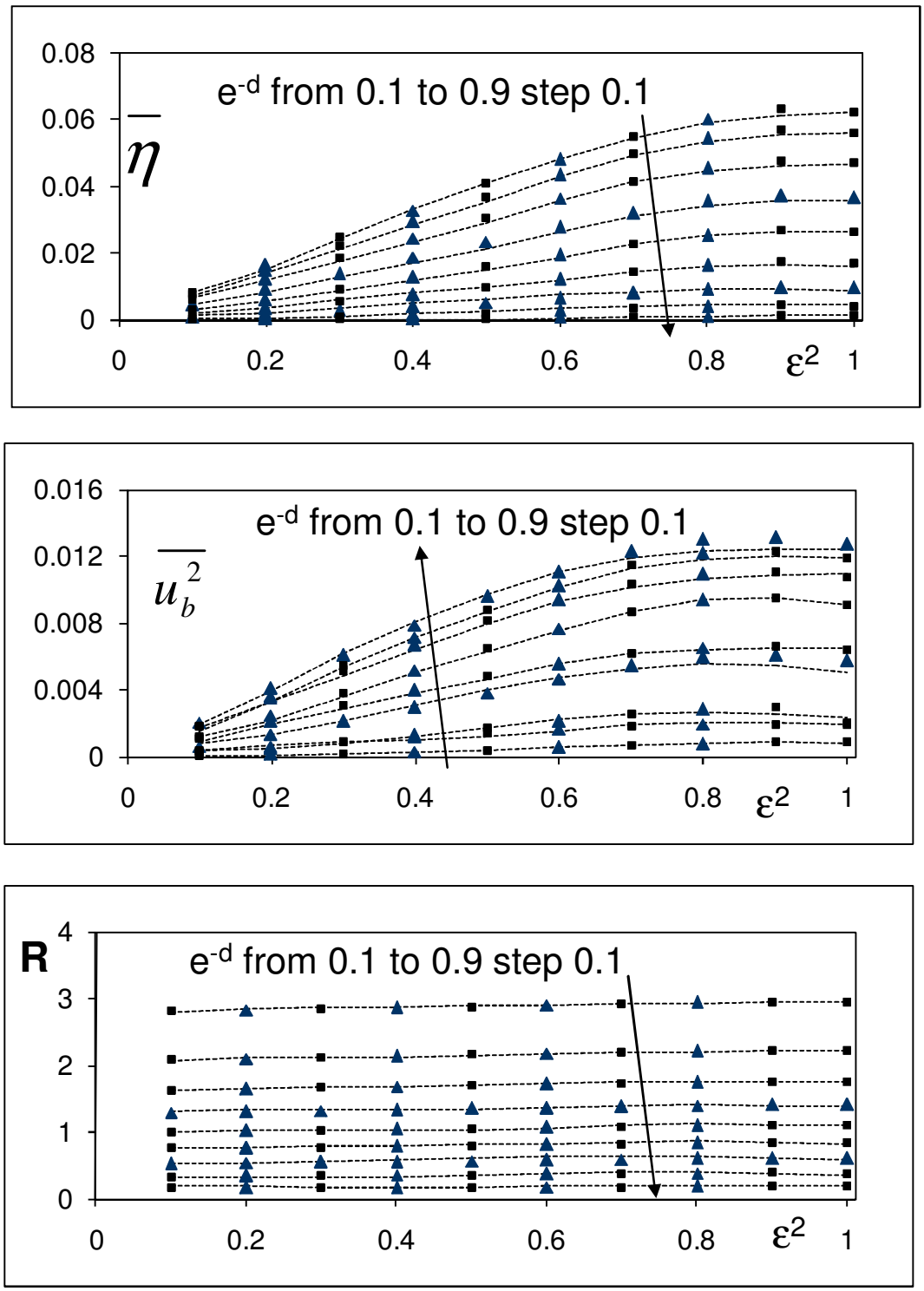

FIGURE 7: Comparison between ANN (dotted lines) and analytical results (symbols) for $\overline{\eta}$, $\overline{u_b^2}$ and *R* at different undisturbed fluid depths and wave nonlinearity parameters. Square symbols used in training phase, and triangle symbols used only for comparison

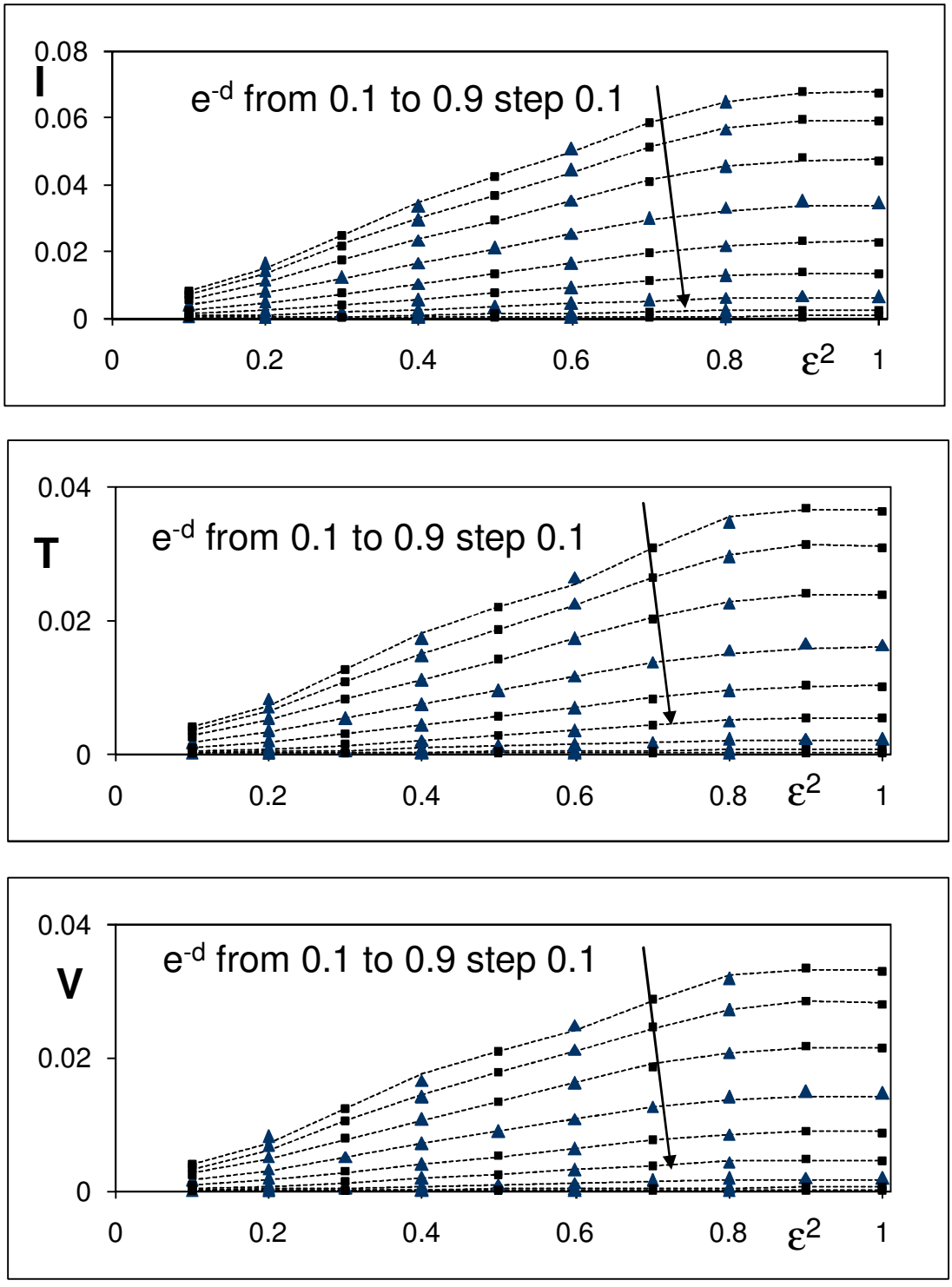

FIGURE 8: Comparison between ANN (dotted lines) and analytical results (symbols) for *I, T* and *V* at different undisturbed fluid depths and wave nonlinearity parameters. Square symbols used in training phase, and triangle symbols used only for comparison

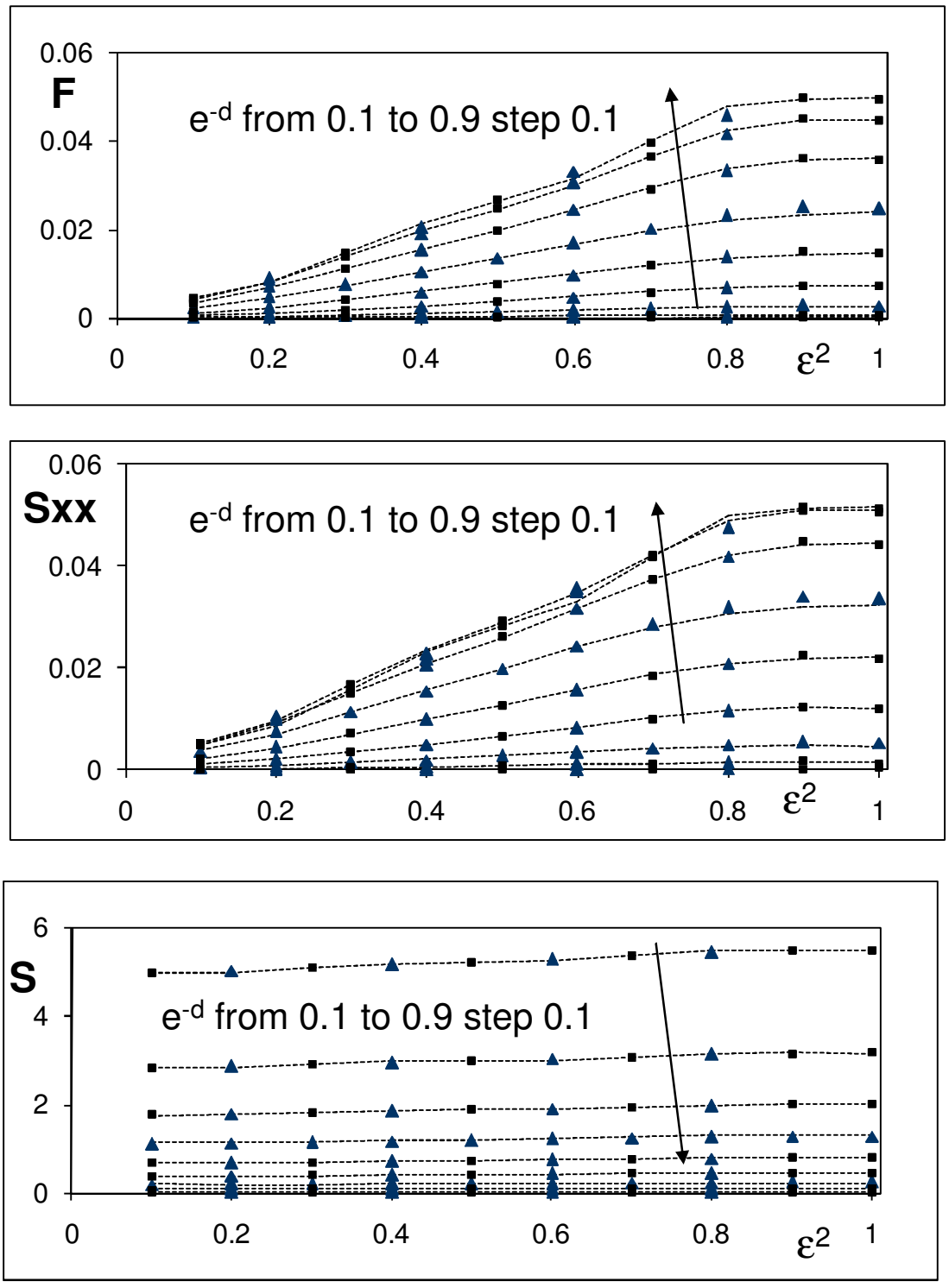

FIGURE 9: Comparison between ANN (dotted lines) and analytical results (symbols) for *F*, S_{xx} and *S* at different undisturbed fluid depths and wave nonlinearity parameters. Square symbols used in training phase, and triangle symbols used only for comparison

8. REFERENCES

1. Abohadima, S., Isobe, M., "Limiting criteria of permanent progressive waves", Coastal Eng., Vol. 44/3, pp. 231-237, 2002.

2. Cokelet, E.D., "Steep gravity waves in water of arbitrary uniform depth", Phil. Trans. R. Soc. London A286, pp. 183-230, 1977.

3. Dean, R.G., "Stream function representation of nonlinear ocean waves", J. Geophys. Res. Vol. 70, pp. 4561-4572, 1965.

4. Dean, R.G., "Evolution and development of water wave theories for engineering application", Vols. I and II, Special Rep. No. 1, US Army Coastal Engin. Res. Center, Fort Belvoir, Virginia, 1974.

5. Chaplin, J.R., "Developments of stream function wave theory", Coastal Eng., Vol. 3, pp. 179-205, 1980.

6. Rienecker M. M. and Fenton J. D., "A Fourier approximation methods for steady water waves", J. Fluid Mech., Vol. 104, pp. 119-137, 1981

7. Longuet-Higgins, M. S. and Fenton, J.D., "On the mass, momentum, energy and circulation of a solitary wave II", Proc. R. Soc. London A340, 471-493, 1974.

8. Schwartz, L.W., "Computer extension and analytic continuation of Stokes's expansion for gravity waves", J. Fluid Mech. Vol. 62, pp. 553-578, 1974.

9. Longuet-Higgins, M. S., "Integral properties of periodic gravity waves of finite amplitude", Proc. R. Soc. London A342, 157-174, 1975.

10. Yamada, H. and Shiotani, T., "On the highest water wave of permanent type", Bull. Disas. Prev. Res. Inst. Kyoto Univ., Vol. 18, Part 2, No. 135, pp. 1-22, 1968.

11. Minns, "Extended Rainfall-Runoff Modeling Using Artificial Neural Networks", Proc. of the 2nd Int. Conference on Hydroinformatics, Zurich, Switzerland, 1996.

12. Kheireldin, K. A., "Neural Network Application for Modeling Hydraulic Characteristics of Severe Contraction", Proc. of the 3rd Int. Conference, Hydroinformatics, Copenhagen - Denmark August 24-26, 1998.

13. Abdeen, M. A. M., "Neural Network Model for predicting Flow Characteristics in Irregular Open Channel", Scientific Journal, Faculty of Engineering-Alexandria University, 40 (4), pp. 539-546, Alexandria, Egypt, 2001.

14. Allam, B. S. M., "Artificial Intelligence Based Predictions of Precautionary Measures for building adjacent to Tunnel Rout during Tunneling Process" Ph.D., 2005.

15. Abdeen, M. A. M., "Development of Artificial Neural Network Model for Simulating the Flow Behavior in Open Channel Infested by Submerged Aquatic Weeds", Journal of Mechanical Science and Technology, KSME Int. J., Vol. 20, No. 10, Soul, Korea, 2006.

16. Mohamed, M. A. M., "Selection of Optimum Lateral Load-Resisting System Using Artificial Neural Networks", M. Sc. Thesis, Faculty of Engineering, Cairo University, Giza, Egypt, 2006.

17. Abdeen, M. A. M., "Predicting the Impact of Vegetations in Open Channels with Different Distributaries' Operations on Water Surface Profile using Artificial Neural Networks", Journal of Mechanical Science and Technology, KSME Int. J., Vol. 22, pp. 1830-1842, Soul, Korea, 2008.

18. Abdeen, M. A. M. and Hodhod, H., "Experimental Investigation and Development of Artificial Neural Network Model for the Properties of Locally Produced Light Weight Aggregate Concrete" Engineering, 2, June 2010, 408-419, Scientific Research Organization, 2010.

19. Hodhod, H. and Abdeen, M. A. M., "Concrete Mix Design Method Based on Experimental Data Base and Predicting the Concrete Behavior Using ANN Technique" Engineering, 2, Augest 2010, 559-572, Scientific Research Organization, 2010.

20. Shin, Y., "Neuralyst^{IM} User's Guide", "Neural Network Technology for Microsoft Excel", Cheshire Engineering Corporation Publisher, 1994